Beyond the Standard Model physics at HERA

Smaïn Kermiche
CPPM, 163 avenue de Luminy, case 907,
13288, Marseille cedex 9, France.
(on behalf of H1 and ZEUS collaborations)

Abstract

The recent results on searches beyond the Standard Model from H1 and ZEUS experiments at HERA are presented. After a brief introduction to the HERA collider running conditions, new results are presented concerning : the limits on the excited fermions masses, the contact interactions scales in different theoretical scenarios, the Leptoquarks coupling and mass limits, constraints on SUSY models with or without R-parity conservation and the events with isolated leptons. At the end an outlook to the HERA future is presented.

1 Introduction

From 1994 to 1997 the HERA ep collider was running with positron (e^+) beam at 27.5 GeV and proton beam at 820 GeV. This gives a center of mass energy of the collision of about 300 GeV. The integrated luminosity of this period is 37 pb^{-1} for H1 and 47 pb^{-1} for ZEUS. In 1998 and a part of 1999[1] HERA ran with electron (e^-) beam of 27.5 GeV and proton beam of 920 GeV, this raises the center of mass energy of the collision to 318 GeV. The integrated luminosity of this period for both the experiments is about 15 pb^{-1}.

All these data allowed the two experiments, H1[1] and ZEUS[2], to get new results concerning the physics beyond the Standard Model. Those results are competitive with, or even better than, those obtained by other collider experiments (e.g. at LEP and TeVatron).

The first part of this paper presents the recent results on the excited fermion searches, i.e excited electrons (e^*), excited neutrinos (ν^*) and excited quarks (q^*). The second part of the paper contains the results obtained on the scale of contact interactions (CI) in different theoretical scenarios. The Leptoquark (LQ) searches are presented in the third part of the paper. Supersymmetry searches performed in the frame of the Minimal Supersymmetric Standard Model (MSSM), with or without R-parity (R_p) conservation, are presented in the fourth part. Before closing with the perspectives of the HERA experiments in the year 2000 and beyond, the recent results concerning the exotic events with isolated leptons are presented. The limits given in all the analyses are obtained with 95% confidence level.

2 Excited fermions

A convincing proof of the substructure of the fermions is a discovery of excited fermions. HERA is well suited to singly produce such particles because of the high energy provided in the collisions. At HERA the excited fermion (f^*) could be produced via the t-channel exchange of a gauge boson (γ, Z or W) and would then decay to a fermion and a boson :

$$e^{\pm} + p \rightarrow f^* + X \rightarrow f + (\gamma, Z^o, W^{\pm}) + X \tag{1}$$

The search is based on the Hagiwara-Komamiya-Zeppenfeld model [3], where the excited fermions are left-right weak isodoublets and have spin 1/2. The Langrangian based on this model takes the form :

$$\mathcal{L} = \frac{1}{\Lambda} f_R^* [f SU(2)_L + f' U(1)_Y + f_s SU(3)_C] f_L \tag{2}$$

Where f, f' and f_s are the coupling constants associated to the SU(2), U(1) and SU(3) gauge groups respectively. Λ is the compositeness scale. Assuming some relations between f, f' and f_s, the production cross sections of the f^*, as well as their branching ratios in the different decay modes, depend only on one parameter (e.g. f/Λ), besides the f^* mass. Constraints on the e^*, ν^* and q^* will be presented under the following conventional assumptions :

[1] In June 1999 HERA switched again to positrons.

- $f = f'$ for the e^* production, to treat equally the SU(2) and the U(1) e^* decays.
- $f = -f'$ for the ν^* production, to allow the radiative decays ($\nu^* \rightarrow \nu\gamma$).
- $fs = 0$ to complement TeVatron searches of pair-produced q^* through their coupling to gluons. Thus q^* are searched here through their decays to electroweak bosons only.

Recent searches for excited fermions at HERA are presented in [4, 5], and earlier results were published in [6, 7]. The following decay modes were studied :

f^*	Decay mode	final state	signature
e^*	$e\gamma$	$e\gamma$	2 electromagnetic clusters
	eZ	eee	3 electromagnetic clusters
		$e\nu\nu$	electromagnetic cluster + track, P_t^{miss}
		eqq	electromagnetic cluster, large E_t^{had} and M^{had}
	νW	$e\nu\nu$	electromagnetic cluster + track, P_t^{miss}
		νqq	P_t^{miss}, large E_t^{had} and M^{had}
ν^*	$\nu\gamma$	$\nu\gamma$	electromagnetic cluster and P_t^{miss}
	νZ	νqq	P_t^{miss}, large E_t^{had} and M^{had}
		$ee\nu$	2 electromagnetic clusters and P_t^{miss}
	eW	eqq	electromagnetic cluster, large E_t^{had} and M^{had}
		$ee\nu$	2 electromagnetic clusters and P_t^{miss}
q^*	$q\gamma$	$q\gamma$	electromagnetic cluster, large E_t^{had}
	qW	$qe\nu$	P_t^{miss}, electromagnetic cluster and large E_t^{had}

Table 1: All the studied channels for the excited fermions. P_t^{miss} is the missing transverse momentum of the event. E_t^{had} is the hadronic transverse energy, M^{had} the hadronic mass.

For all the studied channels we look for high transverse momentum (P_t) objects (electrons, jets) or high missing transverse momentum P_t^{miss} [4, 5]. We describe only one analysed channel and go directly to the results : the production of the e^* and its decay into $e^* \rightarrow e\gamma$. The selection requires high transverse energy electromagnetic clusters. The main background for this channel are the NC DIS (Neutral Current Deep Inelastic Scattering) and the QED Compton. The table below summarizes the mass ranges looked at in both experiments, the efficiencies of signal detection, the number of events obtained and the expected background. We see that the expected Standard Model background is compatible with the observed data.

Analysis	M_{e^*} range (GeV)	efficiency (%)	# data events	# bckgd events
H1	25-250	27-79	223	239 $\pm$ 6
ZEUS	100-250	60-75	60	68 $\pm$ 2

Table 2: The $e^* \rightarrow e\gamma$ channel results for H1 and ZEUS.

The distribution of the $e - \gamma$ invariant mass in the H1 analysis is given in figure 1. We see that data (black points) distribution is compatible with the predicted background (NC DIS and QED Compton) distribution.

Since no excess was observed we extract upper limits on the product of the e^* production cross-section and its branching ratio in this channel. The figure 2 shows the excluded domain (above the curve) for the production of the e^* for the three decay channels : $e^* \rightarrow e\gamma$, $e^* \rightarrow eZ$ and $e^* \rightarrow \nu W$. The best limit is given by the "radiative" channel due to its high efficiency :

$$\sigma \times B_r(e^* \rightarrow e\gamma) <\sim 0.1\,pb\,for\,M_{e^*} = 250\,GeV \tag{3}$$

We also extract mass dependent upper limits on the ratio f/Λ [4]. The figure 3 gives the excluded domains for the different decays for the e^*. We see that this ratio must be less than $10^{-2}\,GeV^{-1}$ for an e^* mass of $250\,GeV$.

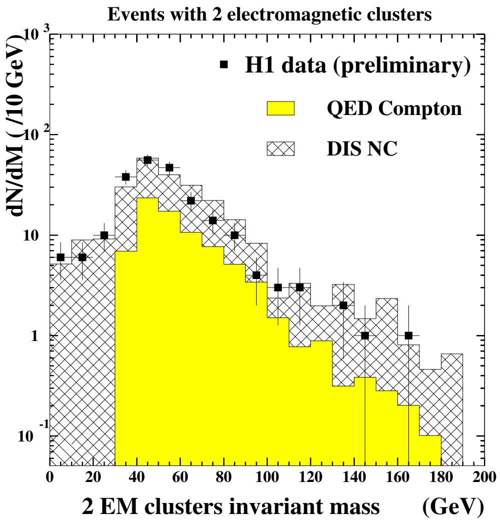

Figure 1: $(e - \gamma)$ invariant mass in the H1 e^* search decaying to $e + \gamma$.

A natural way is to associate it to the excited fermion mass by :

$$\frac{f}{\Lambda} = \frac{1}{M_{f^*}} \tag{4}$$

If we take the assumption $f/\Lambda = 1/M_{e^*}$, we can extract a limit on the e^* mass : $M_{e^*} > 229\,GeV$ [5].

As for the e^*, searches were done for the ν^* and q^* production and decay. The figure 4 shows the exclusion domain on f/Λ for the ν^* from ZEUS search using 98-99 e^-p data. We see that ν^* masses below $100\,GeV$ (resp. $220\,GeV$) are excluded if the f/Λ is higher than $3.5\,10^{-3}\,GeV^{-1}$ (resp. $1.9\,10^{-2}\,GeV^{-1}$). The assumption $f/\Lambda = 1/M_{\nu^*}$ rules out ν^* masses below $161\,GeV$ [5].

The figure 5 shows the exclusion domain on f/Λ for the q^*. We see that q^* masses less than $60\,GeV$ (resp. $230\,GeV$) are excluded if the f/Λ is higher than $0.08\,10^{-2}\,GeV^{-1}$ (resp. $1.9\,10^{-2}\,GeV^{-1}$) [4]. Note that for the case of q^* production via strong interactions and if we assume that $\Lambda = M_{q^*}$, the TeVatron experiments exclude q^* masses below $760\,GeV$. As said above, the HERA results are complementary to the TeVatron results, since we do not need the f_s to produce q^* via electroweak couplings.

The best limits are always given by the "radiative" channels due to their high efficiency.

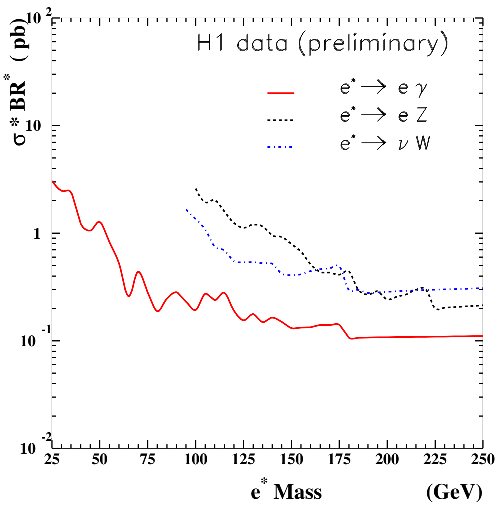

Figure 2: Exclusion domains (above the curve) on the $\sigma \times B_r$ of the e^*.

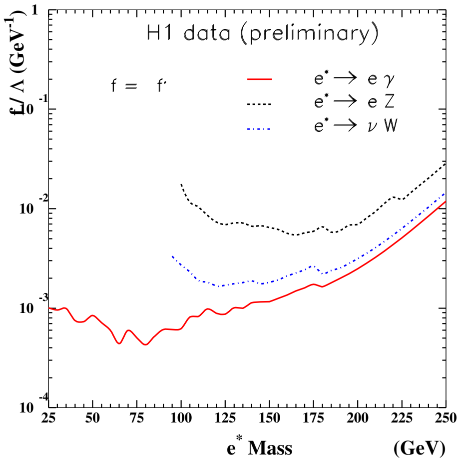

Figure 3: Upper limits on f/Λ as function of the e^* mass.

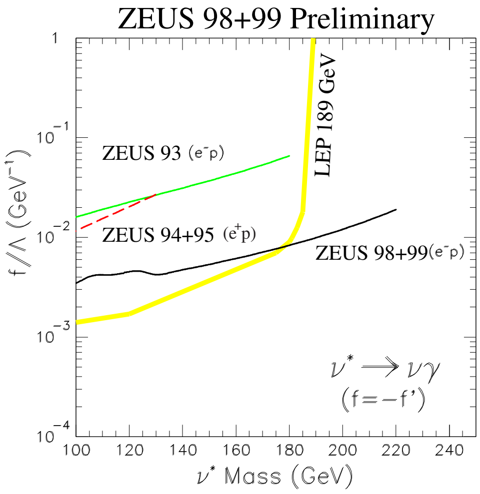

Figure 4: Upper limits on f/Λ as function of the ν^* mass.

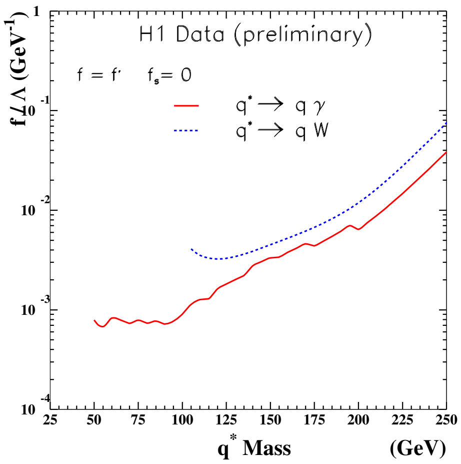

Figure 5: Upper limits on f/Λ as function of the q^* mass.

3 Contact interactions

Contact interactions can parametrize the exchange of particles heavier than the kinematical limit (M >> 300 GeV for HERA case). Those interactions are represented "à la Fermi" by a contact vertex $\pm g^2/\Lambda^2$ (see figure 6). The couplig g of the underlying new interaction is set by convention to $\sqrt{4\pi}$ and Λ denotes its characteristic mass scale.

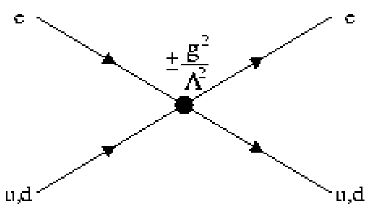

Figure 6: Contact interaction vertex.

Contact Interactions would interfere constructively or destructively with the Standard Model DIS. This would lead to a distortion of the Q^2 spectrum of the observed NC DIS candidate events at high Q^2, as illustrated in figure 7 for a particular CI example.

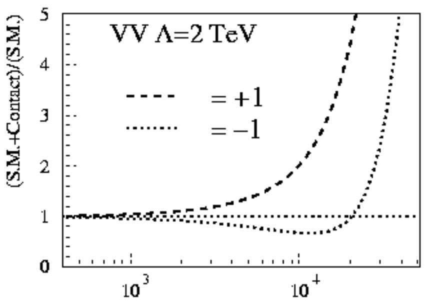

Figure 7: The distortion of the Q^2 distribution due to the introduction of a contact interaction term (in the VV+ and VV− model) with a certain value of Λ.

The most general Lagrangian for the contact interactions reads as ;

$$\mathcal{L}_{CI} = \frac{g^2}{\Lambda^2}\left[\sum_{q=u,d}^{ab=L,R} \epsilon_{ab}^{q}(\bar{e}_a\gamma^{\mu}e_a)(\bar{q}_b\gamma_{\mu}q_b)\right],\ (\epsilon_{ab}^{q} = \pm 1, 0,\ g^2 = 4\pi) \tag{5}$$

In this study only vector terms are considered, since strong limits beyond HERA sensitivity exclude the scalar and tensor terms. With vector terms only, many scenarios (i.e. combinations of the non-vanishing couplings ϵ_{ab}^{q} in the above Lagrangian) can still be considered. The 30 scenarios studied at HERA are defined in table 3. All models can avoid the stringent limits coming from atomic-parity violation searches, and all models except $U2$, $U4$ and $U6$ obey $SU(2)$ symmetry [8, 9].

Since there are no indications for the existence of contact interactions, limits are given on the mass scale. The lower bound on the contact interaction energy scale Λ, in the case of positive (+) and negative (−) interference with the Standard Model, can be obtained e.g. from a χ^2 fit of the observed NC Q^2 distribution to the one expected from Monte-Carlo events mixing Standard Model with a Contact Interaction scenario. Depending on the scenario, the mass scale range is between 1.7 TeV and 5.0 TeV (see table 4 and figure 8) [8, 10].

CI type	ϵ^u_{LL}	ϵ^u_{LR}	ϵ^u_{RL}	ϵ^u_{RR}	ϵ^d_{LL}	ϵ^d_{LR}	ϵ^d_{RL}	ϵ^d_{RR}
VV	+	+	+	+	+	+	+	+
AA	+	−	−	+	+	−	−	+
VA	+	−	+	−	+	−	+	−
X1	+	−	0	0	+	−	0	0
X2	+	0	+	0	+	0	+	0
X3	+	0	0	+	+	0	0	+
X4	0	+	+	0	0	+	+	0
X5	0	+	0	+	0	+	0	+
X6	0	0	+	−	0	0	+	−
U1	+	−	0	0	0	0	0	0
U2	+	0	+	0	0	0	0	0
U3	+	0	0	+	0	0	0	0
U4	0	+	+	0	0	0	0	0
U5	0	+	0	+	0	0	0	0
U6	0	0	+	−	0	0	0	0

Table 3: The contact interaction scenarios studied by ZEUS.

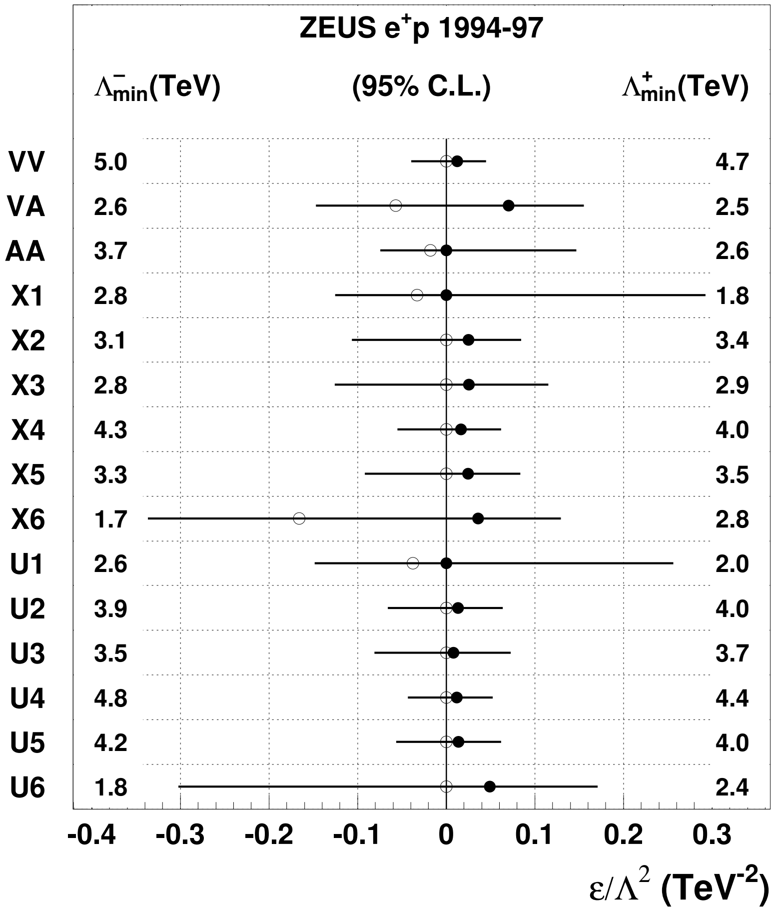

Figure 8: The contact interaction scale limits obtained by ZEUS [8].

CI type	Λ ranges (TeV) at 95% CL [2] ZEUS	H1 (prel)	CDF	D0	ALEPH (prel)	L3 (prel)	OPAL
VV +	4.7	4.5	3.5	4.9	6.7	3.8	4.1
VV −	⇒ 5.0	2.5	5.2	6.1	7.4	5.0	5.7
AA +	2.6	2.0	3.8	4.7	7.4	5.6	6.3
AA −	3.7	3.8	4.8	5.5	8.2	3.5	3.8
VA +	2.8	2.6	−	−	−	−	−
VA −	2.8	2.8	−	−	−	−	−
X1 +	1.8	−	−	3.9	−	−	−
X1 −	2.8	−	−	4.5	−	−	−
X2 +	3.4	−	−	−	−	−	−
X2 −	3.1	−	−	−	−	−	−
X3 +	2.9	−	−	4.2	6.9	4.0	4.4
X3 −	2.8	−	−	5.1	7.7	3.4	3.8
X4 +	4.0	−	−	3.9	2.9	2.9	3.1
X4 −	4.3	−	−	4.4	4.5	4.8	5.5
X5 +	3.5	−	−	−	−	−	−
X5 −	3.3	−	−	−	−	−	−
X6 +	2.8	−	−	4.0	−	−	−
X6 −	⇒ 1.7	−	−	4.3	−	−	−
U1 +	2.0	−	−	−	−	−	−
U1 −	2.6	−	−	−	−	−	−
U2 +	4.0	−	−	−	−	−	−
U2 −	3.9	−	−	−	−	−	−
U3 +	3.7	−	−	−	−	6.1	4.1
U3 −	3.5	−	−	−	−	4.9	5.8
U4 +	4.4	−	−	−	−	2.1	2.3
U4 −	4.8	−	−	−	−	2.9	3.2
U5 +	4.0	−	−	−	−	−	−
U5 −	4.2	−	−	−	−	−	−
U6 +	2.4	−	−	−	−	−	−
U6 −	1.8	−	−	−	−	−	−

Table 4: Contact interaction scale limits obtained by the HERA experiments compared to the results from other experiments (the ⇒ shows the lowest and the highest scale limits).

4 Leptoquarks

Leptoquarks are scalar or vector bosons, coupling to lepton-quark pairs. They appear in Grand Unifying Theories, superstring E6 models and in compositeness. At HERA, Leptoquarks could be resonantly produced via the fusion of the incoming lepton with a quark (antiquark) coming from the proton, as illustrated in figure 9 (right). Recent results on LQs searches at HERA are detailed in [11, 12, 13]

When Leptoquarks decay into $e-q$ or $\nu-q$, they lead to events which are indistinguishable from NC/CC (Charged Current) DIS events at HERA. But the $d\sigma/dx$ distribution must present a narrow resonance (see figure 10) at $x = M_{LQ}^2/s$ where M_{LQ} is the Leptoquark mass.

There is another difference between the Standard Model processes and a Leptoquark production : the $d\sigma/dy$ distribution varies as $1/y^2$ at fixed x for Standard Model NC process while it is flat in y for scalar Leptoquarks and varies as $(1-y)^2$ for vector Leptoquarks (fig 9). Hence, the Leptoquark signal significance can be enhanced by using angular distributions, since $y = 1/2(1+\cos(\theta^*))$ where θ^* is the center of mass decay angle of the LQ, e.g. by optimizing a mass dependant y cut : $y > y_{cut}(M)$.

In the Narrow-Width-Approximation, the cross-section $\sigma(ep \rightarrow LQ \rightarrow eq)$ is as follows :

[2]The LEP limits correspond to data with center of mass energy at 183 GeV.

$$\sigma(ep \to LQ \to eq) \propto \lambda^2 \beta q(x = \frac{M_{LQ}^2}{s}) \tag{6}$$

Where λ is the Yukawa coupling constant at the $LQ - e - q$ vertex, β the branching ratio of the LQ to decay into $e - q$ and $q(x)$ the probability that the struck quark carries the fraction $x = \frac{M_{LQ}^2}{s}$ of the proton momentum.

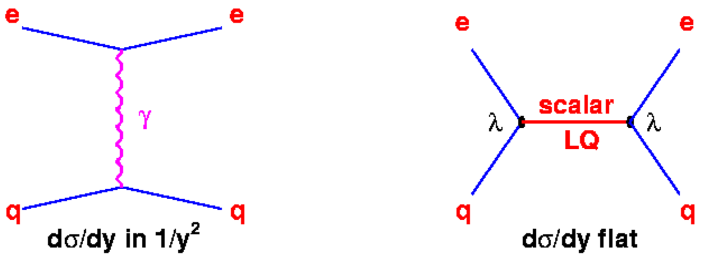

Figure 9: The difference in y distributions between Leptoquark and standard NC DIS events.

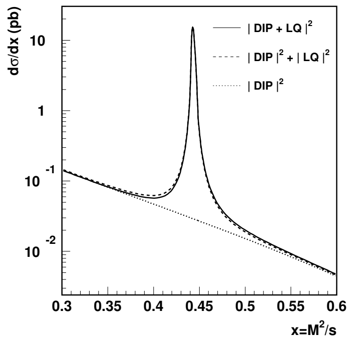

Figure 10: The expected Leptoquark resonance on the $d\sigma/dx$ distribution (for a specific value of M_{LQ}. DIP=DIS).

Hence two approaches can be followed. Working in a specific LQ model, where the branching ratio β is fixed, allows to constrain the Yukawa coupling as a function of the LQ mass. This will be done in subsection 4.1. Alternatively, it's possible to fix the coupling λ and to set mass dependent bounds on the branching ratio β, as will be shown in subsection 4.2. Finally, the case of Lepton Flavour Violating (LFV) LQs will be addressed in subsection 4.3.

4.1 The BRW model analysis

Under different assumptions, Buchmüller, Rückl and Wyler [14] classified the LQs coupling to first generation fermions according to their quantum numbers. Of particular importance at HERA is the fermion number $F = 3B + L$ (B and L denoting the Baryon and Lepton numbers respectively), since LQs with $F = 0$ would be more easily produced with an incident e^+ beam (due to the more favorable parton density since such LQs could be produced via a fusion with a valence quark), while e^- beam would mainly probe $F = 2$ LQs. In the BRW model, the branching ratio β of the LQs to decay into $e - q$ is fixed (1 or 0.5). Figure 11 shows the different types of scalar LQs contained in the BRW model.

The invariant mass distribution of the selected events by H1, in the case of NC DIS selection, is shown in the figure 12 before and after the application of the optimized mass dependent y_{cut} mentioned above. The excess arround the mass value of 200 GeV due to the 1994-1996 data is still there, it becomes less significant if we add the 1997 data [11].

F = 2	prod/decay			β	F = 0	prod/decay			β
$^{-1/3}S_0^*$	$e_R^+\bar{u}_R$	$\rightarrow$	$e^+\bar{u}$	1/2	$^{-5/3}S_{1/2}^*$	$e_L^+u_L$	$\rightarrow$	e^+u	1
		$\rightarrow$	$\bar{\nu}_e\bar{d}$	1/2		$e_R^+u_R$	$\rightarrow$	e^+u	1
	$e_L^+\bar{u}_L$	$\rightarrow$	$e^+\bar{u}$	1	$^{-2/3}S_{1/2}^*$	$e_L^+d_L$	$\rightarrow$	e^+d	1
$^{-4/3}\tilde{S}_0^*$	$e_L^+\bar{d}_L$	$\rightarrow$	$e^+\bar{d}$	1	$^{-2/3}\tilde{S}_{1/2}^*$	$e_R^+d_R$	$\rightarrow$	e^+d	1
$^{-4/3}S_1^*$	$e_R^+\bar{d}_R$	$\rightarrow$	$e^+\bar{d}$	1					
$^{-1/3}S_1^*$	$e_R^+\bar{u}_R$	$\rightarrow$	$e^+\bar{u}$	1/2					
		$\rightarrow$	$\bar{\nu}_e\bar{d}$	1/2					

Figure 11: The Scalar Leptoquarks in the BRW model.

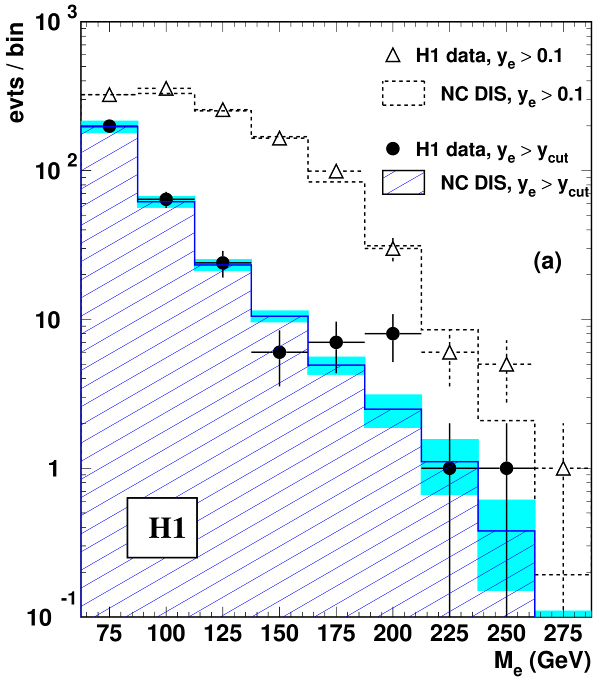

Figure 12: Mass distribution for NC DIS events.

Since no significant excess has been seen on the data, upper limits on the coupling constant λ can be set [11]. We see those limits for different scalar Leptoquark types in figure 13 (the domain above the curves is excluded). We see that the best limits are given by Leptoquarks coupling to valence quarks (i.e $F = 0$ LQs) due to higher probability to find high x values for such quarks. And in this category, the $S_{1/2,R}$ Leptoquark gives the best limit since it couples to both u and d quarks.

The Leptoquark mass limit we can extract for a Yukawa coupling constant of the order of the electomagnetic coupling constant ($\lambda \simeq \sqrt{4\pi\alpha_{em}}$) is : $M_{LQ} > 275\,(284)\,GeV$ for scalar (vector) LQs (figure 13). For $F = 2$ LQs, and for electroweak couplings, ZEUS experiment excludes masses below 290 GeV (figure 14) using 98-99 e^-p data [13].

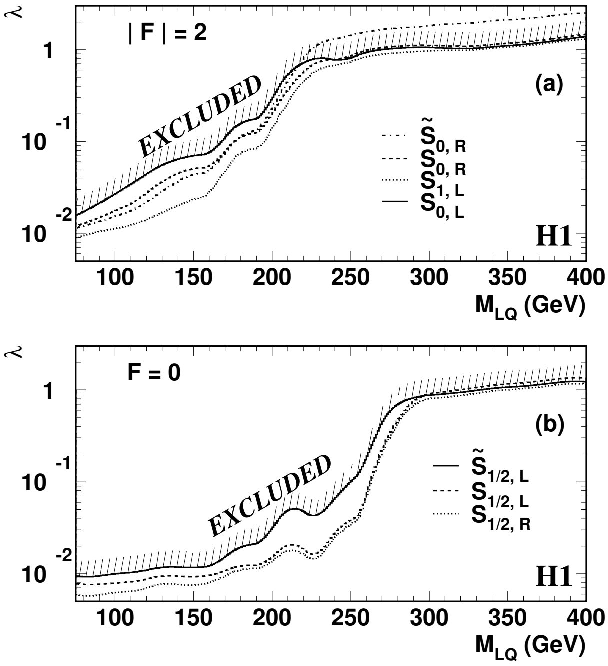

Figure 13: Upper limits on the Yukawa coupling λ as a function of the LQ mass in the BRW model, obtained from the analysis of $\sim 37pb^{-1}$ of e^+p data.

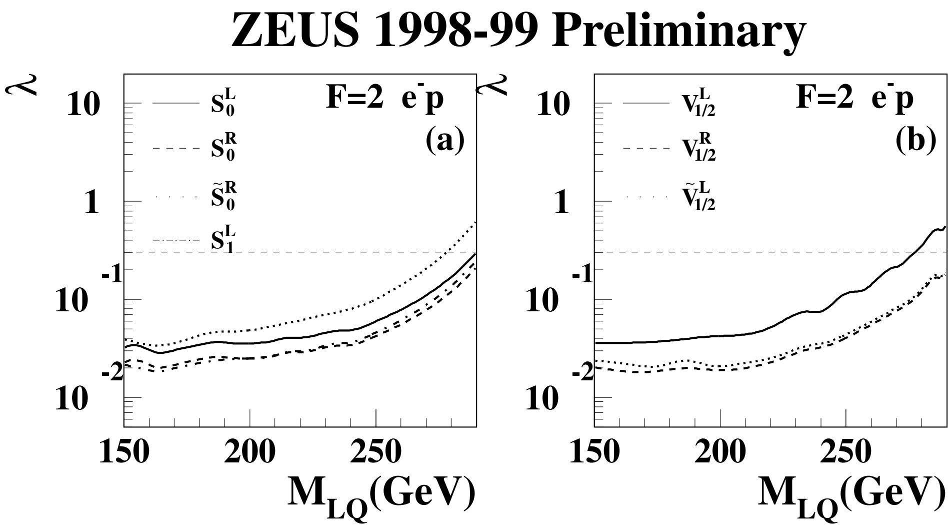

Figure 14: Upper limits on the Yukawa coupling λ as a function of the LQ mass in the BRW model for F=2 LQs, obtained from the analysis of $\sim 15pb^{-1}$ of e^-p data.

4.2 The free branching ratio analysis

We now move away from the BRW model and consider "generic" LQs for which the branching ratio β to decay into eq is not fixed and considered as a free parameter.

The figure 15 shows the excluded domain as a function of the Leptoquark mass, for different assumptions of Yukawa coupling constant λ [11]. We see that the HERA experiments cover new domain which was not covered by the other experiments. For example for a value of $\lambda = 0.1$ (i.e. a coupling three times less than the electromagnetic coupling) HERA is in competition with the TeVatron results. We see also that HERA has still a high discovery potential for even small λ, provided that β is not too large.

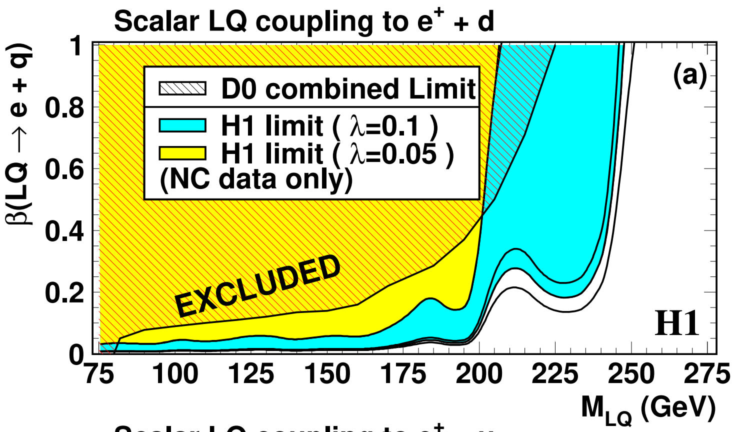

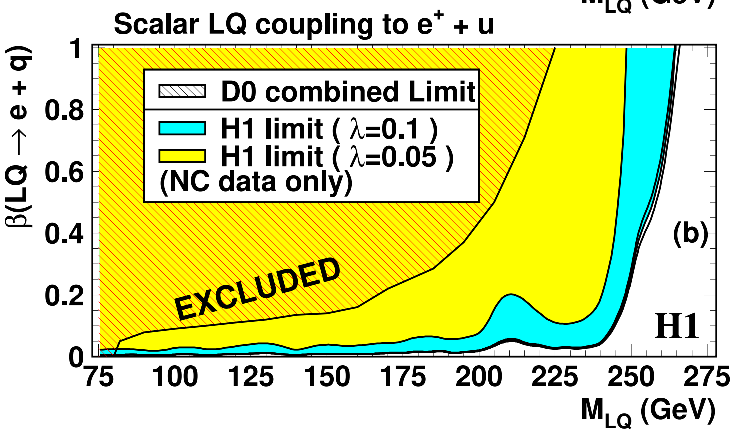

Figure 15: Mass dependent exclusion limits on the branching ratio $\beta(LQ \rightarrow eq)$ for scalar leptoquarks produced by (a) e^+d and (b) e^+u fusion. Two exclusion regions corresponding to $\lambda = 0.1$ and $\lambda = 0.05$ are represented as greyed areas. For $\lambda = 0.1$, the error bands on the exclusion limits in (a) and (b) illustrate the sensitivity to d and u quark densities respectively (see text). The $D\emptyset$ limit is also shown as hatched region.

4.3 The case of Leptoquarks decaying with lepton flavour violation (LFV)

We now considere LQs which couple both to $e - q$ and $\tau - q$ pairs. Limits are set [11, 15] for the Yukawa coupling constants taking into account that the Leptoquarks could decay by changing the flavour of the lepton[3]:

$$LQ \rightarrow e + q \ (\beta_e) \tag{7}$$
$$LQ \rightarrow \tau + q \ (\beta_\tau) \tag{8}$$

For an electromagnetic coupling strenght ($\lambda_e = 0.3$) and for $\beta_e = 0.1$ and $\beta_\tau = 0.9$, $M_{LQ} < 275\,GeV$ is excluded for Leptoquarks coupling to e^+u (see figure 16). If $\beta_e \simeq 0.1$ and β_τ high, HERA has still a high discovery potential where the TeVatron limit are below 100 GeV [16, 17].

[3] See also the "Isolated Leptons" section for the muon case.

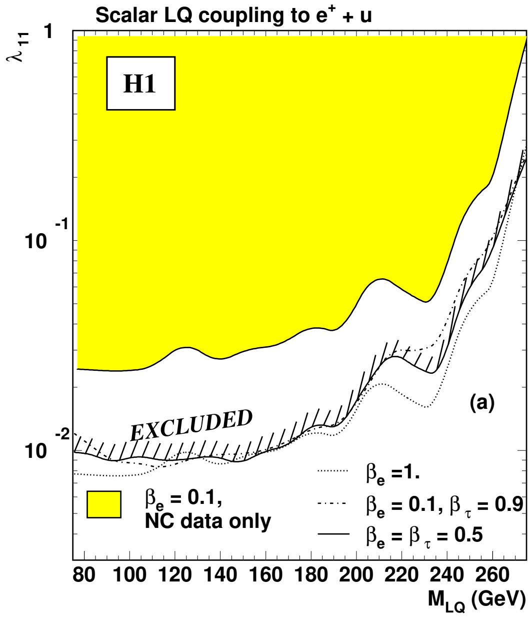

Figure 16: λ_e limits in case of LFV Leptoquarks.

5 SUSY: R_p violation/conservation

The Supersymmetry potential has two parts, one MSSM part conserving the "R-Parity" (R_P) and one part violating it :

$$W_{SUSY} = W_{MSSM} + W_{\not R_P} \tag{9}$$

The R_P is a multiplicative quantum number defined by :

$$R_p = (-1)^{3B+L+2S} \tag{10}$$

Where B, L and S are the Baryon number, the Lepton number and the Spin respectively.

5.1 R_P conservation searches

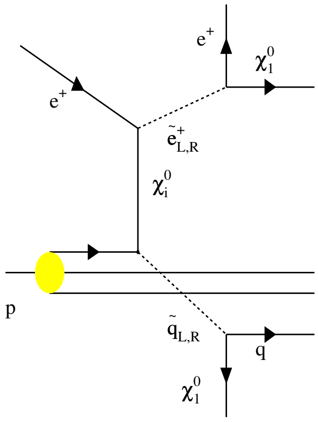

Figure 17: One example of s-particles production in the MSSM R_P conservation.

In this case the superparticles are produced by pairs (see the figure 17), and the LSP (Lightest Supersymmetric Particle) χ^o_1 is stable and undetected at the final state : $\tilde{e}(\tilde{q}) \rightarrow e(q) + \chi^o_1$

The cross section of such process depends mainly on the sum of the slepton and squark masses : $M_{\tilde{e}} + M_{\tilde{q}}$. Such searches have been perfomed and published in [18, 19].

Since no evidence of squark production at HERA was observed for the R_P conserving channels, we can give limits [18]. In this case, the limits are given in the plane $(M_{\tilde{e}}, M_{\tilde{q}})$ using different assumptions on the MSSM parameters. The figure 18 shows the exclusion plane for $\tan\beta = 1.41$, $\mu = -100 GeV$, and for two values of $M_{\chi_1^\circ}$ (35 GeV and 50 GeV). The figure shows also the special case of the up-squark. We see that for a neutralino of mass $M_{\chi_1^\circ} = 40\,GeV$ the region where $(M_{\tilde{e}} + M_{\tilde{q}})/2 < 77\,GeV$ is excluded[4].

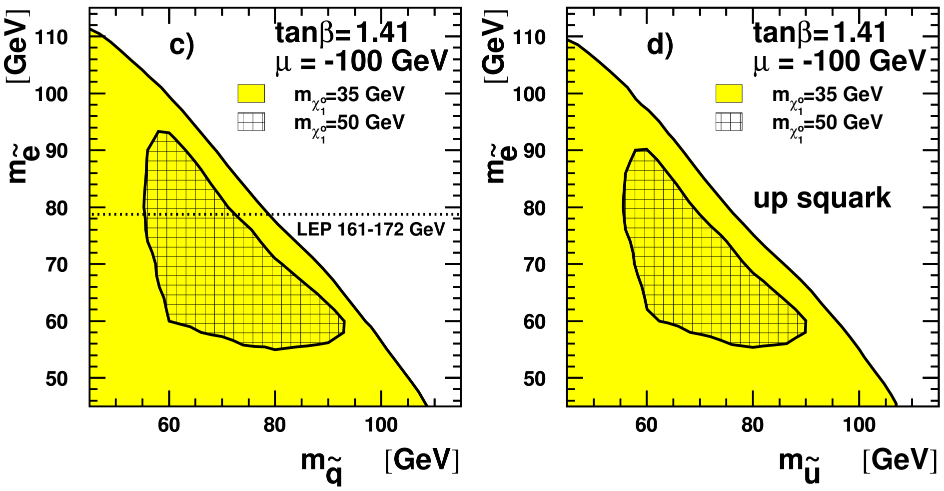

Figure 18: $M_{\tilde{e}} + M_{\tilde{q}}$ limits for a chosen set of MSSM parameters.

5.2 R_P violation searches

The potential giving the R_P violation is the following :

$$W_{\not R_P} = \lambda_{ijk} L_i L_j \bar{E}_k + \lambda'_{ijk} L_i Q_j \bar{D}_k + \lambda''_{ijk} \bar{U}_i \bar{D}_j \bar{D}_k \tag{11}$$

where ijk are generation indices of the superfields L, Q, E, D and U. The L and Q are left-handed doublets while $\bar{E}$, $\bar{D}$ and $\bar{U}$ are right-handed singlet superfields for charged leptons, down and up-type quarks, respectively. The part of the potential which interests us at HERA is the second one, coupling squarks to lepton-quark pairs. Through such λ'_{1jk} couplings squarks can be singly produced, and then decay in two ways, the R_P violating decay and the gauge decay (see figures 19 and 20).

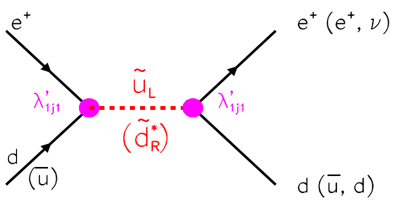

Figure 19: Squark decaying by R_P violation.

[4]Those limits are now superseeded by the latest LEP2 results.

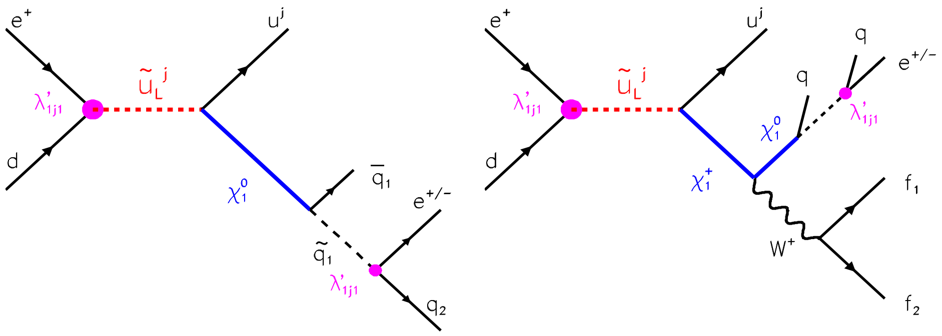

Figure 20: Example gauge decays of squarks into a neutralino χ^0 or a chargino χ^+, followed by the subsequent decay of the χ.

In the case of positron beam (the case of our analysed data), e^+ probes mainly the λ'_{1j1} couplings :

$$e^+ d \longrightarrow \tilde{u_L}, \tilde{c_L}, \tilde{t_L} \tag{12}$$

The search for such a signal has been performed in many possible final states in [20]. More recent searches are presented in [21, 22].

Since no evidence of squark production at HERA was observed for the R_P violating channels, We can give limits [22]. In this case, the limits are given on the coupling constants as function of the squark mass. These limits depend on the MSSM parameters determining the mixing of the neutralinos and charginos. Four cases have been considered for this set of parameters, and the corresponding results are shown in figure 21. For $\lambda'_{1j1} = 0.3$ squark masses up to $M_{\tilde{q}} \simeq 275\ GeV$ are excluded.

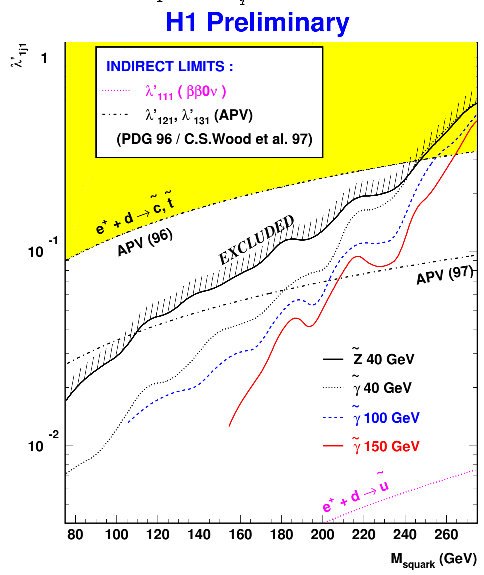

Figure 21: Mass dependant upper limits on λ'_{1j1} under different assumptions on the MSSM parameters.

6 Isolated leptons

Since 1994 HERA experiments observe unusual events with isolated leptons (electrons or muons) and with high missing transverse momentum (P_t^{miss}) [15, 23, 24, 25]. Figure 22 represents one of them, where the isolated lepton is a muon.

$$e^+p \to \mu^+X$$

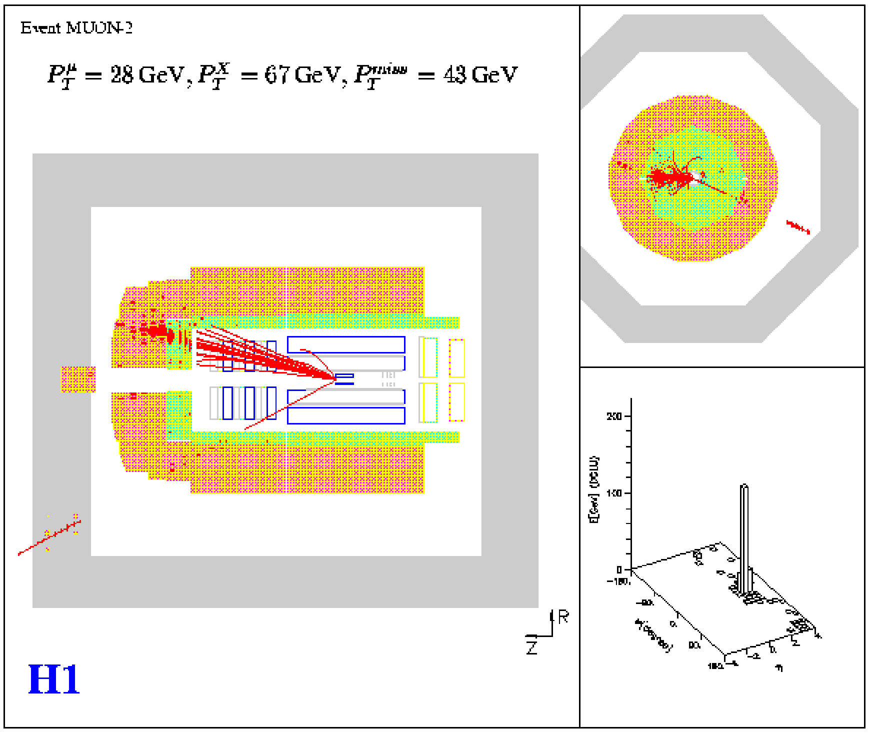

Figure 22: An isolated muon candidate in H1.

The characteristics of such events are a well isolated lepton, a missing P_t and an acoplanarity between the isolated lepton and the hadronic system.

The table 5 presents the findings of both the experiments H1 and ZEUS. H1 sees a muon excess (5 muons candidates for 94-97 data) while ZEUS does not. We need more luminosity to well understand such events.

	electrons		muons	
	Data	Expected	Data	Expected
94-97 e^+				
H1 (37 pb^{-1})	1 e^-	2.4 ± 0.5	5 μ ($2\mu^+, 2\mu^-, 1\mu$)	0.8 ± 0.2
ZEUS (47 pb^{-1})	3 e^+	3.5 ± 0.7	0 μ	2.0 ± 0.4
98-99 e^-				
H1 (13.6 pb^{-1})	0 e	1.0 ± 0.2	0 μ	0.4 ± 0.1
ZEUS (16.0 pb^{-1})	2 e^+	0.8 ± 0.4	0 μ	0.8 ± 0.1

Table 5: The isolated lepton candidates and the SM expectations.

The figure 23 shows a comparison between the main Standard Model processes (W production and $\gamma\gamma$ processes) which could give such a final state, and the isolated lepton events of H1 (P_t^{had} versus (Isolated lepton-ν) transverse mass). The Monte Carlo luminosity is 500 times the data one. We see that μ_3 event is compatible with a W production ($e^+p \to e^+\mu^-X$), but the μ_1,μ_2 and μ_4 are unlikely W production or $\gamma\gamma$ (due to high P_t^{had}). The μ_5 is less well constrained.

The interpretation of such events beyond the Standard Model such as LFV Leptoquark production, fails, since the kinematics are incompatible [11].

It has been proposed [22, 26] that these events could be due to a resonantly produced stop decaying into sbottom + W. Indeed the kinematics of the "H1 muon events" is not incompatible with such a process, for $M_{\tilde{t}_1} = 200\,GeV$ and $M_{\tilde{b}_1} = 90 - 120\,GeV$

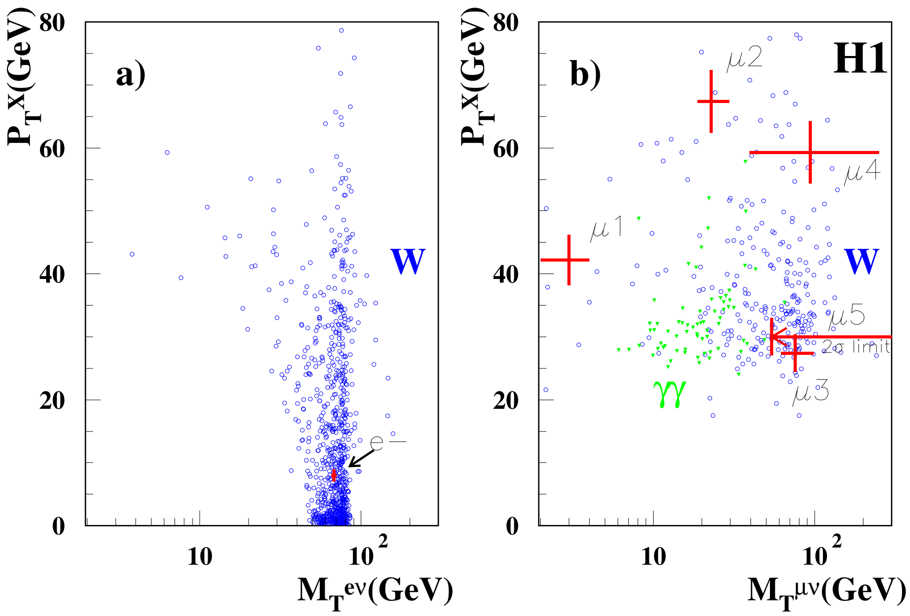

Figure 23: Comparison of the isolated lepton kinematics with the Standard Model events.

7 HERA in the future

As we have seen, HERA experiments have obtained competitive results on the beyond Standard Model searches compared with other collider experiments. We have seen also that HERA still has discovery potentials. This is why the coming data are crucial for physics. HERA will accumulate about $50pb^{-1}$ from now up to May 2000. To start a high luminosity regime, on spring 2001, a shutdown of about 9 months is scheduled to install the luminosity upgrade. HERA will accumulate up to $\simeq$ 2005, with this high luminosity regime, about $1fb^{-1}$.

References

[1] H1 Collaboration, I. Abt et al., DESY Preprint 93-103 (July 1993).

[2] ZEUS Collaboration, M. Derrick et al., Status report (October 1993), DESY.

[3] K.Hagiwara et al. Z. Phys. C29, 115 (1985).

[4] H1 Collaboration, C. Adloff et al., ICHEP'98 Contrib. paper, abstract 581.

[5] ZEUS Collaboration, J. Breitweg et al, EPS'99 Contrib. paper, abstract 555.

[6] H1 Collaboration, S. Aid et al., Nucl. Phys. B483 (1997) 44.

[7] ZEUS Collaboration, J. Breitweg et al, Z. Phys. C76 (1997) 631.

[8] ZEUS Collaboration, J. Breitweg et al., preprint DESY-99-058, May 1999.

[9] A. F. Zarnecki, DESY 99-074 (hep-ph/9904334) and references therin.

[10] H1 Collaboration, S. Aid et al, Phys. Lett. B353 (1995) 578.
H1 Collaboration, C. Adloff et al, ICHEP'98 proceedings, Abstract 584.
H1 Collaboration, C. Adloff et al, EPS'99 Contrib. paper, Abstract 157 f.

[11] H1 Collaboration, C. Adloff et al., Preprint DESY-99-081, June 1999 (to appear in Eur.Phys.J. C)

[12] ZEUS Collaboration, J. Breitweg et al, ICHEP'98 Contrib. paper, Abstract 754.

[13] ZEUS Collaboration, J. Breitweg et al, EPS'99 Contrib. paper, Abstract 546 and 552.

[14] W. Buchmüller, R. Rückl and D. Wyler, Phys. Lett. B191 (1987) 442.
Erratum: Phys. Lett. B448 (1999) 320.

[15] ZEUS Collaboration, J. Breitweg et al, EPS'99 Contrib. paper, Abstract 551.

[16] CDF Collaboration, F. Abe et al, Phys. Rev. Lett. 78 (1997) 2906.

[17] D0 Collaboration, B. Abbott et al, Phys. Rev. Lett. 81 (1998) 38.

[18] ZEUS Collaboration, J. Breitweg et al, Phys. Lett. B434 (1998) 214.

[19] H1 Collaboration, S. Aid et al., Phys. Lett. B380 (1996) 461.

[20] H1 Collaboration, S. Aid et al., Z.Phys. C71 (1996) 211.

[21] ZEUS Collaboration, J. Breitweg et al, EPS'99 Contrib. paper, Abstract 548.

[22] H1 Collaboration, S. Aid et al., ICHEP'98 Contrib. paper, Abstract 580.

[23] H1 Collaboration, C. Adloff et al., Eur. Phys. Jour. C5 (1998) 575.

[24] H1 Collaboration, C. Adloff et al., EPS'99 Contrib. paper, Abstract 157.

[25] ZEUS Collaboration, J. Breitweg et al, preprint DESY-99-054, July 1999.

[26] T. Kon, T. Matsushita, T. Kobayashi, Mod. Phys. Lett. A12 (1997) 3143.